



# Photosynthetic semiconductor biohybrids for solar-driven biocatalysis

Stefano Cestellos-Blanco<sup>1</sup>, Hao Zhang<sup>2</sup>, Ji Min Kim<sup>1</sup>, Yue-xiao Shen<sup>2</sup> and Peidong Yang<sup>1,2,3,4</sup>

**Photosynthetic semiconductor biohybrids integrate the best attributes of biological whole-cell catalysts and semiconducting nanomaterials. Enzymatic machinery enveloped in its native cellular environment offers exquisite product selectivity and low substrate activation barriers while semiconducting nanomaterials harvest light energy stably and efficiently. In this Review Article, we illustrate the evolution and advances of photosynthetic semiconductor biohybrids focusing on the conversion of CO<sub>2</sub> to value-added chemicals. We begin by considering the potential of this nascent field to meet global energy challenges while comparing it to alternate approaches. This is followed by a discussion of the advantageous coupling of electrotrophic organisms with light-active electrodes for solar-to-chemical conversion. We detail the dynamic investigation of photosensitized micro-organisms creating direct light harvesting within unicellular organisms while describing complementary developments in the understanding of charge transfer mechanisms and cytoprotection. Lastly, we focus on trends and improvements needed in photosynthetic semiconductor biohybrids in order to address future challenges and enhance their widespread adoption for the production of solar chemicals.**

Societal and industrial development has yielded a plethora of benefits for a quickly expanding and interconnected global population. While our quality of life has vastly improved over the past century, it has come at a cost exemplified by depletion of finite energy reserves as well as release of harmful greenhouse gases into the atmosphere contributing to increasingly erratic climatic patterns<sup>1</sup>. The consumption of hydrocarbon fuels is further aggravated, as the carbon ends up as dilute and nearly inert CO<sub>2</sub>. In order to prevent further environmental deterioration and secure a lasting energy source, we must find a deployable strategy to simultaneously tap into renewable energy and close the carbon cycle.

Regarding renewable energy, sunlight provides an unparalleled abundance of energy on Earth; one hour of solar irradiation matches our yearly global consumption<sup>2,3</sup>. It is no coincidence that Earth's biomass is largely derived from solar energy. Although electricity obtained from photovoltaics has gained a foothold in the energy landscape, carbon-based liquid drop-in fuels remain critically important for their stability and high energy density. Overcoming our global energy challenge will undoubtedly require the development of strategies to harvest and store solar power<sup>4</sup>.

Nature has provided a blueprint in photosynthesis for capturing and storing solar energy in chemical bonds<sup>5</sup>. However, our energy demands realistically outmatch the short-term capability of this natural process<sup>6</sup>. Attempts to directly use plant biomass have resulted in noncompetitive economics and deviation of resources from agricultural needs<sup>7</sup>. Overall, nature does not perform satisfactorily at solar capture, as conventional crops only have a 1–2% solar-to-biomass conversion efficiency<sup>8</sup>.

By contrast, inorganic materials, in particular devices consisting of doped semiconductors, have benefited from decades of intense research and technological development. Commercial silicon-based photovoltaic cells customarily reach 20% solar-to-electricity conversion rates even securing profitability<sup>9</sup>. Additionally, photovoltaic-driven electrolysis could achieve at least 10–12% solar energy to

water splitting efficiency<sup>10,11</sup>. Advantageously, inorganic light harvesters do not suffer from photodamage and can be engineered to scale to specific light environments. Biological organisms, on the other hand, require a stable light source, and an appropriate climatic environment<sup>12</sup>. Although the benefits of inorganic materials for light capture are significant, they do not hold the upper hand over biology in regard to CO<sub>2</sub> fixation. Most semiconducting materials are not suitable catalysts for CO<sub>2</sub> reduction<sup>13</sup>. Therefore, light capture and charge transfer to CO<sub>2</sub> must occur on different platforms. Despite the fact that catalysts for CO<sub>2</sub> reduction have progressed expediently, the catalytic understanding necessary for solar-to-chemical conversion is not fully mature<sup>14</sup>. Photoelectrochemical reactors for CO<sub>2</sub> reduction have produced mostly C<sub>1</sub> compounds such as carbon monoxide, methane, methanol and formate<sup>15–17</sup>. These devices also suffer from low product selectivity, often employ rare metals and long-term stability has not been entirely fulfilled. By comparison, biological organisms engage an army of enzymes and reductive pathways to produce long-chain hydrocarbons from naturally available constituents including CO<sub>2</sub>, H<sub>2</sub>O and N<sub>2</sub>. Enzymes and proteins within the metabolic pathways of cells benefit from an ingrained building code in genetic information and are repaired and replicated as necessary. For these reasons, the combination of inorganic light-harvesters and whole-cell biocatalysts would exploit the most salient attributes of each component. In particular, semiconducting nanomaterials are highly configurable, pair well with cellular organisms due to similar lengths scales and provide adequate light capture.

In this Review Article, we lay out the progression of photosynthetic semiconductor biohybrids on three fronts: (i) biocatalyst integration in photoelectrochemical devices, (ii) whole-cell micro-organisms photosensitized with light-harvesting nanoparticles and accompanying understanding of charge transfer mechanisms, (iii) and lastly cytoprotective strategies to enhance whole-cell photosensitization. Finally, we illustrate notable areas for improvement in this field and discuss potential approaches to address these

<sup>1</sup>Department of Materials Science and Engineering, University of California, Berkeley, CA, USA. <sup>2</sup>Department of Chemistry, University of California, Berkeley, CA, USA. <sup>3</sup>Materials Sciences Division, Lawrence Berkeley National Laboratory, Berkeley, CA, USA. <sup>4</sup>Kavli Energy NanoSciences Institute at the University of California, Berkeley, CA, USA. ✉e-mail: [p\\_yang@berkeley.edu](mailto:p_yang@berkeley.edu)

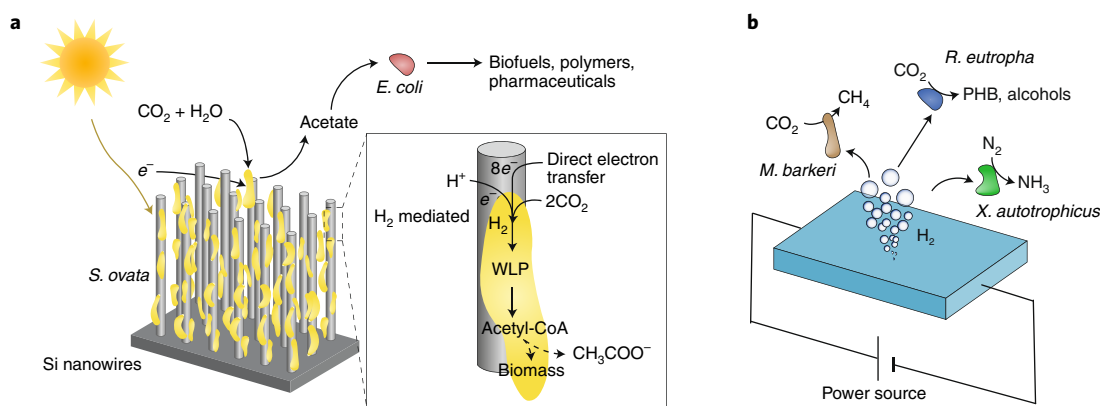


**Fig. 1 | Photoelectrochemical semiconductor biohybrids. a**, *S. ovata* loaded on light-harvesting nanowire arrays undertake  $\text{CO}_2$ -to-acetate conversion. Genetically engineered *E. coli* upgrades acetate to value-added products. The inset shows the WLP leading to acetogenesis. **b**, A contrasting strategy consists of water electrolysis producing  $\text{H}_2$ . Microorganisms utilize  $\text{H}_2$  as a feedstock to generate  $\text{CH}_4$ ,  $\text{NH}_3$ , biofuels and PHB.

challenges. Overall, we illustrate how a biohybrid catalytic approach could establish the efficient and stable production of liquid fuels from sunlight—a liquid sunlight approach<sup>18</sup>.

### Photoelectrochemical semiconductor biohybrids

Economic expansion has rendered the worldwide carbon flux unidirectional with  $\text{CO}_2$  serving as a final carbon sink following the utilization of fossil fuels. Nature is the single biggest contributor to atmospheric  $\text{CO}_2$  fixation through photosynthesis, however our energy demands vastly outmatch nature's time-scale. Artificial photosynthesis aims to mimic the conversion of  $\text{CO}_2$  into value-added carbon products powered by solar energy<sup>19</sup>. Recent advances in semiconductor materials enable broadband light absorption and high photoconversion rates<sup>20</sup>. Photoelectrochemical (PEC) systems integrating light-harvesting semiconducting materials with catalysts primed for  $\text{CO}_2$  reduction have been documented<sup>21,22</sup>. These systems obtain light energy from semiconducting electrode materials or external light-harvesters and couple the photoreaction with appropriate catalysts that bind and transfer electrons to  $\text{CO}_2$  (ref. 14). Nevertheless, even among state-of-the-art  $\text{CO}_2$  catalysts, selectivity for products other than CO or formic acid remains poor<sup>23</sup>. Additionally, Faradaic efficiencies, a benchmark of catalyst selectivity, for  $\text{C}_{2+}$  chemicals are low. Natural organisms have evolved to rely on enzymes to convert  $\text{CO}_2$  to upgradeable intermediates such as acetyl-CoA and pyruvic acid with exquisite selectivity<sup>24</sup>. Enzymes undertake conformational changes to create local hydrophobic environments and promote steric effects to aid in reaction selectivity<sup>25</sup>. Additionally, dangling amino acid residues mediate electron and proton transfers while stabilizing reactive intermediates<sup>26</sup>. Electron transfer between purified enzymes and electrodes has been studied for conversion of chemical energy to electricity<sup>27</sup>,  $\text{CO}_2$  fixation<sup>28</sup>, water splitting<sup>29</sup> and chemical sensing<sup>30</sup>. This approach leverages the product specificity of enzymatic catalysts, and also circumvents product and energy losses due to secondary biomass accumulation. However, combining proteins in vitro within a PEC setup results in stability issues<sup>31</sup>. Enzymes inhabit unique protective environments and often operate synergistically with other proteins and organelles; therefore, coupling purified enzymes with electrodes is nontrivial. Additionally, connecting enzymes to an electrode often requires technically advanced procedures<sup>32</sup>. In light of these complications, exploiting the enzymatic machinery within whole cells could improve stability by preserving innate replication and healing mechanisms<sup>33</sup>. Pairing whole-cell biocatalysts with artificial light-capturing PEC systems could enhance product selectivity and lower energetic barriers of  $\text{CO}_2$  activation.

At the outset, the integration of whole-cell biocatalysts with inorganic electrodes forged multiple avenues for powering microbial metabolism for the synthesis of desired chemicals from  $\text{CO}_2$  and  $\text{H}_2\text{O}$  (refs. 34,35). An early demonstration of microbial electrosynthesis consisted of pairing acetogen *Sporomusa ovata* with a graphite cathode<sup>36</sup>. The electrons transferred to *S. ovata* facilitated the reduction of  $\text{CO}_2$  into organic carbon compounds via the Wood–Ljungdahl pathway (WLP)<sup>37</sup>. Conveniently, acetate is a by-product of the WLP as  $\text{CO}_2$  is converted to acetyl-CoA, which is oxidized to acetate in ATP phosphorylation. The Faradaic efficiency of acetate, as calculated by accounting for the fraction of electrons passed through the cathode consumed to produce acetate, was found to be over 85%. After the initial demonstration of microbial electrosynthesis for the production of multicarbon organic compounds from  $\text{CO}_2$ , different approaches have been undertaken to improve performance and product selection including optimization of electrode geometry<sup>38</sup>, electrode surface engineering<sup>39,40</sup> as well as bacteria adaptation<sup>41</sup>, enrichment<sup>42</sup> and genetic modification<sup>43</sup>.

Liu et al. realized solar-to-chemical microbial electrosynthesis by loading *S. ovata* into a light-harvesting semiconductor nanowire PEC cell (Fig. 1a)<sup>44</sup>. Si and  $\text{TiO}_2$  photoactive nanowires captured simulated sunlight and provided *S. ovata* with electrons to drive  $\text{CO}_2$  reduction. The Si nanowire substrate can accommodate higher loading of *S. ovata* than planar substrates. The high-surface-area nanowire platform allows for greater interface between the bacteria and cathode, which enhances current density—a measure of the rate of  $\text{CO}_2$  fixation. Additionally, the nanowire electrodes create a local anaerobic environment that maintains the viability of *S. ovata* even with oxygenic headspace gas. Significantly, the *S. ovata*–nanowire biohybrids were completely operated under simulated sunlight without an external bias achieving a peak  $\text{CO}_2$ -reducing photocurrent of  $-0.35 \text{ mA cm}^{-2}$  with circa 90% Faradaic efficiency at an operating overpotential of 0.2 V. The overall energy conversion efficiency under simulated sunlight was 0.38%. The bio-produced acetate was upgraded to value-added multicarbon products, such as *n*-butanol, polyhydroxybutyrate (PHB) and isoprenoid by genetically altered *Escherichia coli* (*E. coli*) (Fig. 1a). Altogether this study demonstrates the ability of semiconductor biohybrids to replicate photosynthesis by combining  $\text{CO}_2$ , sunlight and  $\text{H}_2\text{O}$  into fuels, polymers and pharmaceuticals.

Autotrophic organisms may also consume  $\text{H}_2$  as a form of reducing equivalent<sup>34,45,46</sup>. Therefore,  $\text{H}_2$  can be considered as a charge mediator to facilitate microbial electrosynthesis. In this case the cathode may be used as an electrolyser to reduce water (Fig. 1b). Accordingly, cathodic materials with appropriate  $\text{H}_2$  catalytic

activity at neutral pH need to be selected. Nichols et al. paired platinum- and nickel-based  $H_2$  electrocatalysts with *Methanosarcina barkeri* (*M. barkeri*) to convert  $CO_2$  to methane<sup>47</sup>. The Faradaic efficiency of this device was tabulated at 81% over three days with a  $-0.29\text{ mA cm}^{-2}$  current density. Additionally, the electrodes were substituted with an indium phosphide photocathode and a titanium dioxide photoanode to create an unassisted solar-driven system with 74% Faradaic efficiency. Moreover, Liu et al. illustrated that cobalt-based  $H_2$  catalysts can be used in conjunction with genetically engineered *Ralstonia eutropha* (*R. eutropha*) (later renamed *Cupriavidus necator*) to produce biomass, PHB and alcohols from  $CO_2$  (ref. <sup>48</sup>). The biocompatible cobalt phosphorous electrodes produce  $H_2$  and  $O_2$  under low driving voltage while minimizing reactive oxygen species (ROS) generation, which had previously inhibited microbial metabolism<sup>43,49</sup>. The authors report that their system could achieve 7.6% and 7.1% solar-to-chemical efficiencies for PHB and fusel alcohols, respectively, if paired with a photovoltaic device. Notably, these cobalt-based electrodes were used in a following study with *Xanthobacter autotrophicus* (*X. autotrophicus*) to fix  $N_2$  gas into  $NH_3$  and nitrogenous biomass<sup>50</sup>. Nevertheless, the low solubility of  $H_2$  in aqueous media as a mediator limits the throughput of microbial electrosynthesis. Recently, Rodrigues et al. employed a biocompatible perfluorocarbon nanoemulsion as an  $H_2$  carrier thus increasing the solubility of  $H_2$  (ref. <sup>51</sup>). This strategy was successfully combined with *S. ovata*, helping the model system achieve a current density of  $2\text{ mA cm}^{-2}$  with near 100% Faradaic efficiency.

### Whole-cell photosensitization

A key aim of the nascent field of biohybrid photocatalysis has been to expand beyond the limitations set forth by PEC systems. These systems, which are best suited for purely inorganic photocatalysis, may require a strong light flux and variable pH conditions incompatible with living organisms. Furthermore, extracellular electron transfer can be a bottleneck limiting the rate of photoreduction by bacteria. While the interface between inorganic cathodic materials and bacteria is actively under investigation, small changes in the local environment can have deleterious effects. For instance, current density of a biohybrid PEC device is restricted by the resulting local change in pH near the cathode, which creates an inhospitable environment for microorganisms. Leaching of toxic metals from the electrodes as well as ROS generation present an engineering challenge. For these reasons, it has been a pressing need to devise a semiconductor–cell interface that overcomes these limitations.

Several unicellular autotrophic microorganisms have evolved light-absorbing centres thus housing both light-energy harvesting and  $CO_2$ -fixation centres. Cyanobacteria in particular are capable of undertaking complete photosynthesis by converting  $CO_2$  to carbohydrates with sunlight. Efforts have been devoted to genetically engineering cyanobacteria to produce biofuels as well as to process their raw biomass<sup>52</sup>. These photosynthetic organisms offer insight on the biology required for cells to use photoexcited reducing equivalents and indicate that intracellular machinery may be powered by light. Utschig et al. combined photosystems I (PSI) and II (PSII) in cyanobacteria thylakoid membranes with Pt nanoparticle catalysts for solar hydrogen production<sup>53</sup>. Furthermore, Brown et al. achieved  $N_2$  to  $NH_3$  reduction by pairing nitrogenase with light-activated CdS nanorods<sup>54</sup>. These studies indicate that isolated cellular components can be linked to abiotic nanostructures and can even be impelled with light. Nevertheless, associations of purified proteins with inorganic nanomaterials may suffer from a lack of durability. In addition, the carbon-fixation pathways of non-photosynthetic organisms, particularly the WLP, are energetically favourable for the production of chemicals<sup>55</sup>.

Sakimoto et al. enhanced a model non-photosynthetic acetogen *Moorella thermoacetica* with light-absorbing cadmium sulfide (CdS) nanoparticles (Fig. 2a)<sup>56</sup>. Although the precipitation of

inorganic nanoparticles within microorganisms is a well-known protective response to toxic metal ions<sup>57</sup>, the ability of these nanoparticles to absorb light within the host microorganism had not been thoroughly studied. Cysteine desulfhyrase, an enzyme found in *M. thermoacetica* among other microorganisms, produces sulfide from cysteine<sup>58,59</sup>. Sulfide reacts with metal ions, such as  $Cd^{2+}$  introduced to cell culture media, to form high-quality and homogenous CdS nanoparticles. The nanoparticles are primarily anchored in the cell membrane. Most interestingly, illumination drives autotrophic  $CO_2$  conversion to multicarbon acetate in the *M. thermoacetica*–CdS constructs. *M. thermoacetica* consumes the photogenerated reducing equivalents produced by illuminated CdS nanoparticles to power their innate  $CO_2$ -fixing metabolism. Under the WLP  $CO_2$  is enzymatically reduced to acetyl-CoA, which is then either used for protein biosynthesis or oxidized to acetate to obtain ATP. Cysteine not only provides a source of sulfur but also serves as a hole scavenger. Charge separation at the inorganic nanoparticle interface is aided by the oxidation of cysteine to cystine. Further spectroscopic examination of the charge transfer and uptake pathway is needed in order to elucidate the molecular mechanism of this photoreaction. Overall, the *M. thermoacetica*–CdS constructs generated acetate from  $CO_2$  in three days under low-intensity simulated sunlight with  $2.44 \pm 0.62\%$  overall quantum yield (Table 1). The discovery of photosensitized microorganisms for  $CO_2$  reduction actualizes a largely unexplored line of investigation. Although quantum dots and nanostructures have been introduced in cells for fluorescent labelling<sup>60</sup> and drug delivery<sup>61</sup> for well over two decades, light-absorbing nanostructures had not been used to drive reactions inside of cells. Photosensitized microorganisms offer an additional strategy for photocatalysis and also present an opportunity for investigating the interface between light-activated nanomaterials and whole-cell organisms.

Further self-photosensitization with CdS nanoparticles of varied microorganisms for photocatalysis has been reported. Wang et al. presented a biohybrid system consisting of *Rhodospseudomonas palustris* and CdS (ref. <sup>62</sup>). While *R. palustris* is a non-sulfur, purple photosynthetic bacterium, it still requires a source of reducing equivalents as it produces bacteriochlorophyll protein—a type II bacterial light reaction centre. *R. palustris* fixes  $CO_2$  through the Calvin cycle into biomass, carotenoids and PHB under illumination. Photosensitization of *R. palustris* with CdS promotes the production of these  $C_{2+}$  compounds. Overall, the photosynthetic efficiency of *R. palustris*–CdS is 1.67% higher than the natural control (Table 1). Moreover, Chen and colleagues complemented denitrifying bacterium *Thiobacillus denitrificans* with self-precipitated CdS nanoparticles<sup>63</sup>. *T. denitrificans*–CdS use photogenerated reducing equivalents to reduce  $NO_3^-$  to  $N_2O$ . The authors also confirmed that the relative transcript abundance of genes encoding for denitrifying proteins is upregulated in biohybrid *T. denitrificans*–CdS after illumination.

CdS nanoparticles, while an effective semiconducting nanomaterial, may limit the efficiency of the  $CO_2$  photoreduction as they induce oxidative stress and are thus cytotoxic to anaerobic bacteria like *M. thermoacetica*<sup>64,65</sup>. Furthermore, they present an environmental hazard that limits their applicability in  $CO_2$  recycling<sup>66</sup>. Gold nanoclusters (AuNCs) are sub-3 nm nanoparticles consisting of a precise number of atoms bound together by organic ligands<sup>67</sup>. These AuNCs have garnered interest due to their unique optical and electronic properties based on both the number of atoms and overall arrangement<sup>68</sup>. In addition, choice of surface ligands enables exquisite control over their biochemical properties<sup>69</sup>. In particular, thiol-protected AuNCs displaying chromophore-like discrete energy states have been applied in catalysis<sup>70</sup>, optics<sup>71</sup> and for solar energy harvesting<sup>72,73</sup>.  $Au_{22}(SG)_{18}$  (SG, glutathione) is both water soluble and exhibits high luminescence, which makes it a candidate for microorganism photosensitization<sup>74</sup>. Zhang et al. document that



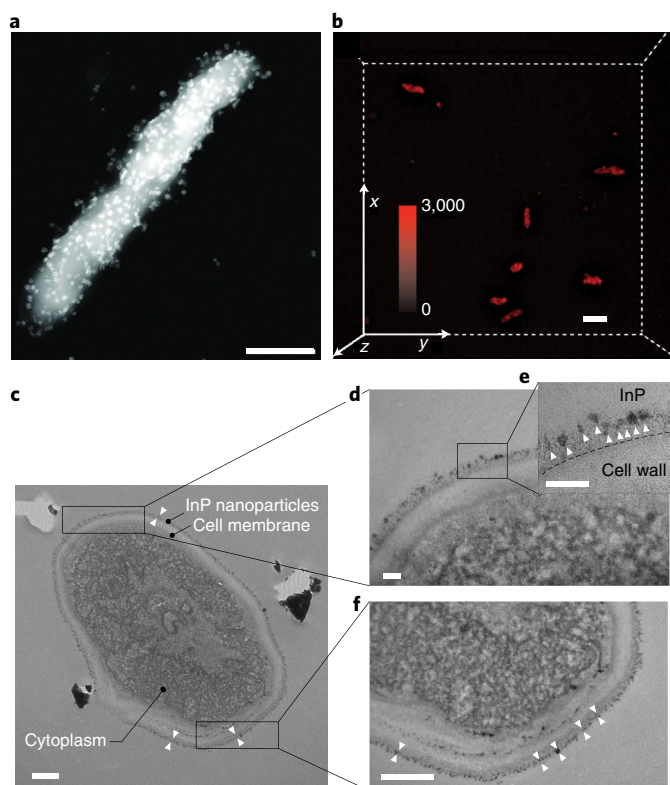


**Fig. 2 | Methods for visualization of light-active nanoparticles on cells.**

**a**, High-angle annular dark field STEM image illustrating the association of CdS nanoparticles on the membrane of *M. thermoacetica* (scale bar, 500 nm). **b**, Fluorescence intensity measured by structure illumination microscopy confirms the presence of AuNCs on *M. thermoacetica* (scale bar, 2  $\mu$ m). **c**, Cross-sectional TEM image of *S. cerevisiae*-InP hybrid with InP assembled on the cell membrane (scale bar, 500 nm). **d-f**, Series of magnified images depict detail of the InP nanoparticle association on the cell membrane (scale bars, 100 nm (**d,e**); 500 nm (**f**)). Figure adapted with permission from ref. <sup>56</sup>, AAAS (**a**); ref. <sup>75</sup>, Springer Nature Ltd (**b**); ref. <sup>82</sup>, AAAS (**c-f**).

over 90% of  $\text{Au}_{22}(\text{SG})_{18}$  is taken up by *M. thermoacetica* when added to a pre-exponential culture and  $\text{Au}_{22}(\text{SG})_{18}$  retains its luminescence over a period of seven days (Fig. 2b)<sup>75</sup>. Importantly,  $\text{Au}_{22}(\text{SG})_{18}$  does not hinder cell proliferation at optimal concentrations. In fact, in contrast with CdS,  $\text{Au}_{22}(\text{SG})_{18}$  quenches photoexcited radicals including ROS. This advantageous effect translates to higher viability of *M. thermoacetica*-AuNCs cultures than in *M. thermoacetica*-CdS. The diminutive size of AuNCs allows for increased interface between the light-absorbing particle and cell machinery. The improved interface and biocompatibility in *M. thermoacetica*-AuNCs resulted in an appreciably higher rate of acetate production from  $\text{CO}_2$  under simulated sunlight. The overall quantum yield of *M. thermoacetica*-AuNCs was  $2.86 \pm 0.38\%$  compared with  $2.44 \pm 0.62\%$  for *M. thermoacetica*-CdS (Table 1).

Photosensitization of *M. thermoacetica* with CdS nanoparticles or AuNCs offers an approach for combining the selectivity and replication of biology with the light-harvesting capability of inorganic semiconductors for photocatalysis<sup>76</sup>. However, autotrophic bacteria are disadvantaged by slow reproduction times, high oxygen sensitivity and are limited to few exogenous products<sup>77</sup>. Organisms such as *E. coli* and yeast serve as workhorses of synthetic biology, as significant progress has been made to tailor their metabolic pathways<sup>78,79</sup>. Therefore, devising of strategies to augment these microorganisms with light-absorption capabilities would signify an important

advance in the field. Wei and co-workers report on the enhancement of genetically engineered *E. coli* with CdS nanoparticles<sup>80</sup>. Interestingly, the authors utilize PbrR, a membrane-bound protein with cysteine residues that selectively adsorbs lead and cadmium ions to precipitate CdS nanoparticles. As cysteine desulfhydrase, the enzyme responsible for sulfide production and CdS precipitation in *M. thermoacetica* is not present in all bacterial strains, PbrR and similar proteins could be exploited to generate nanoparticles in a wider spectrum of cells. The *E. coli* is genetically engineered to synthesize [NiFe]-hydrogenase. [NiFe]-hydrogenase has been previously linked to PSI used as a photosensitizer for light-driven generation of  $\text{H}_2$  (ref. <sup>81</sup>). In the study led by Wei et al. the *E. coli*-CdS constructs produce hydrogen under illumination. This solar-to-chemical scheme is, however, hampered by the inherent oxygen sensitivity of hydrogenase.

Moreover, Guo and colleagues functionalized genetically engineered yeast with light-absorbing indium phosphide (InP) nanoparticles (Fig. 2c-f)<sup>82</sup>. *Saccharomyces cerevisiae* operates heterotrophically utilizing hexose sugar as a substrate for biomass, energy and target metabolites. Low yields of sugar to target metabolites, exemplarily shikimic acid, a precursor molecule in biomanufacturing, can be attributed to the loss of carbon as  $\text{CO}_2$  in the oxidative generation of NADPH. However, NADPH is needed as a reducing equivalent in a host of cell functions. Deletion of the pentose phosphate pathway in *S. cerevisiae* decreases the availability of NADPH but also halts the loss of carbon as  $\text{CO}_2$ . The authors claim that InP nanoparticles enable the regeneration of NADPH without the oxidation of hexose through the pentose phosphate pathway in genetically engineered *S. cerevisiae*. Therefore, *S. cerevisiae* decorated with broadly absorbing InP nanoparticles can consume photogenerated NADPH, which increases carbon flux toward shikimic acid production. *S. cerevisiae*-InP hybrids effectively decouple biosynthesis and NADPH regeneration. These highlighted studies involving *E. coli* and yeast, respectively provide blueprints for combining workhorse microorganisms with light-absorbing nanoparticles for the solar-powered production of fuels and fine chemicals.

Although the field encompassing the coupling of whole-cell organisms with light-absorbing nanomaterials for photocatalysis is rapidly expanding, there is a lack in systematically matching the bandgap energy of light-absorbing nanoparticles with the redox potential of target enzymes.

Ding et al. report recently on the synthesis of semiconducting nanoparticles with finely tuned bandgaps for biohybrid photocatalysis<sup>83</sup>. Seven different core-shell quantum dots (QDs) were produced, each with a different bandgap energy for wide-ranging utilization of the solar spectrum. The surface chemistries of the QDs with CdS, CdSe, InP and  $\text{Cu}_2\text{ZnSnS}_4$  cores were tailored to biocompatibly bind to enzymes in *Azotobacter vinelandii* and *C. necator*. The authors found that a zinc sulfide shell has a strong binding affinity to histidine-tagged MoFe nitrogenase and Fe-S clusters in hydrogenase in cell lysates. They further modified the surface of the QDs with zwitterion cysteine in order to improve the association of QDs with the bacteria. Finally, the *C. necator*-QD constructs provide a platform for the solar generation of a plethora of carbon-based products including methyl ketones, butanediol, ethylene, PHB and propanol. *A. vinelandii*-QD hybrids were used to generate  $\text{NH}_3/\text{H}_2$  and formic acid. Together, these results indicate that the tunability of electronic properties as well as the modifiable surface chemistry of nanomaterials can be leveraged to operate synergistically with biological catalysts. Figure 3 and Table 1 offer an overview and summary with quantum yield metrics of reported cell-photo-sensitizer pairings.

### Charge transfer

A fundamental question arises from the growing field of whole-cell photosensitization: how do cells use reducing equivalents derived

**Table 1 | Representative summary of photosensitized microorganisms**

Host organism	Photosensitizer (bandgap, eV)	Substrate/product	Quantum yield	Reference
<i>M. thermoacetica</i>	CdS (2.51)	CO <sub>2</sub> /acetate	2.44 ± 0.62% with simulated sunlight 52 ± 17% with 435–485 nm LED	<sup>56</sup>
<i>R. palustris</i>	CdS	CO <sub>2</sub> /PHB, carotenoids	1.67% increase in photosynthetic efficiency with fluorescent lightbulbs	<sup>62</sup>
<i>T. denitrificans</i>	CdS (2.54)	NO <sub>3</sub> <sup>−</sup> /N <sub>2</sub> O	2.0 ± 0.2% with 395nm LED	<sup>63</sup>
<i>M. thermoacetica</i>	Au <sub>22</sub> (SG) <sub>18</sub>	CO <sub>2</sub> /acetate	2.86 ± 0.38% with simulated sunlight	<sup>75</sup>
<i>E. coli</i>	CdS (2.92)	H <sub>2</sub> O/H <sub>2</sub>	-	<sup>80</sup>
<i>S. cerevisiae</i>	InP	Hexose/shikimic acid	1.58 ± 0.05% with cold-white LED	<sup>82</sup>
<i>A. vinelandii</i>	CdS@ZnS nanoparticles (2.90–2.98) CdSe@ZnS nanoparticles (2.17–2.48) InP@ZnS (1.72) Cu <sub>2</sub> ZnSnS <sub>4</sub> @ZnS(1.55)	N <sub>2</sub> & H <sub>2</sub> O/NH <sub>3</sub> & H <sub>2</sub> CO <sub>2</sub> /formic acid	13.1% combined for NH <sub>3</sub> & H <sub>2</sub> with CdS@ZnS	<sup>83</sup>
<i>C. necator</i>	CdS@ZnS nanoparticles (2.90–2.98) CdSe@ZnS nanoparticles (2.17–2.48) InP@ZnS (1.72)	CO <sub>2</sub> /methyl ketones, butanediol, ethylene, PHB, propanol	~0.6% for ethylene with CdS@ZnS	<sup>83</sup>

Provided data includes organism, photosensitizer, substrate/product combinations. Quantum yield is represented by the ratio of electrons used to reduce a substrate to a final product and the total input photon flux as per ref. <sup>56</sup> (for example, from CO<sub>2</sub> to acetate: QY% =  $\frac{8e^- \times \text{mol acetate}}{\text{mol total photons}} \times 100\%$ ). This calculation is modified as necessary in further studies.

from photoexcited nanoparticles? Charge transfer studies performed on bioelectrochemical systems provide a knowledge base. Although autotrophic bacteria can commonly use H<sub>2</sub> as a source of energy, many such organisms have also evolved the ability to establish direct electrical contact. Electroactive bacteria can transport electrons to and from a poised electrode<sup>84</sup>. The charge transfer mechanism in particular between an anode and charge-donating bacteria has been investigated<sup>85,86</sup>. Membrane-bound proteins can shuttle electrons across the cell membrane<sup>87</sup>. Surface-displayed cytochromes and flavins are commonly involved in this process but evolving research constantly yields new information on charge uptake pathways<sup>88</sup>. The oxidation of inorganic mineral oxides mediated by electrostatic interactions is carried out by surface-displayed haemoproteins. Exemplarily, Fukushima et al. report that extracellular electron transfer protein MtrF, a terminal protein in cytochrome *c* from *Shewanella oneidensis* MR-1 binds to mineral oxides by creating a three-dimensional, positively charged pocket of specific residues (Fig. 4a)<sup>89</sup>. Moreover, electrotrophic bacteria may also secrete proteins and small molecules that act as redox shuttles as well as extracellular polymers, coined as microbial nanowires<sup>90,91</sup>. Cryoelectron microscopy was used to discern the structure of microbial nanowires in *Geobacter sulfurreducens* responsible for long-range electron transport (Fig. 4b)<sup>92</sup>. It was determined that the nanowires consist of hexahaem cytochrome OmcS with haems assembled within 3–6 Å of each other (Fig. 4c). Electron conduction occurs through the core of the filaments over the tightly packed metal-cluster haems.

The platform established by cell-nanoparticle hybrids may serve to study the charge transfer between biotic/inorganic interfaces spectroscopically. Namely, the translucent and light-activated biohybrid samples facilitate in situ observation by spectroscopic means. Transmittance-based transient absorption (TA) and time-resolved infrared spectroscopy (TRIR) were employed to elucidate charge carrier lifetimes in *M. thermoacetica*-CdS (Fig. 4d)<sup>93</sup>. The photoexcited reducing equivalents may be taken up by hydrogenase or directly as electrons by membrane-bound proteins. Through appropriate experimental design, the biochemical activity of proteins involved with charge uptake was correlated with charge carrier lifetimes. *M. thermoacetica*-CdS constructs were incubated with hydrogen pre-photosynthesis for varying lengths of time in order to ramp up hydrogenase activity. The rate of acetate production was higher in the first three hours for those samples with no hydrogen incubation, but the average rate of acetate production was higher in the samples with the longest hydrogen incubation time. TA results

showed that bare CdS had the slowest decay kinetics followed by *M. thermoacetica*-CdS with no hydrogen incubation, while *M. thermoacetica*-CdS with hydrogen incubation exhibited the fastest decay. These observations indicate that a CdS-to-hydrogenase electron transfer pathway may be established. Interestingly, the TRIR spectra highlight a change in vibrational range of CO and CN double and triple bonds corresponding to amino acid residues. These changes occur on the same timescale as the TA signal. While the spectral changes in the TRIR spectra occur in hydrogen and non-hydrogen incubated samples, slight differences point to two charge uptake mechanisms. Photoexcited electrons feed directly into proteins accelerating acetate production in samples with limited hydrogenase activity but cannot maintain long-term metabolic activity due to lack of high energy reducing equivalents. Whereas a CdS-to-hydrogenase electron transfer pathway is established in samples with sufficient hydrogenase activity to produce high energy reducing equivalents.

Kornienko et al. proposed photoinduced charge transfer mechanisms in photosensitized whole-cells based on spectroscopic differences between CdS-containing cells and a control group. Nevertheless, further investigation to identify and quantify the proteins involved during CdS-induced photosynthesis would provide crucial insights. Zhang and colleagues probed the proteome and metabolome of hybrid cells by high-sensitivity mass spectrometry techniques<sup>94</sup>. Firstly, they found that membrane-bound proteins ferredoxin, flavoprotein and NADH dehydrogenase are upregulated in *M. thermoacetica*-CdS, indicating that these proteins are responsible for electron uptake (Fig. 4e). These electrons are further integrated into bacterial metabolism by shuttling menaquinones where they are used to reduce CO<sub>2</sub> to acetyl-CoA with CO dehydrogenase and acetyl synthase. It is worth remarking that upregulation of ATP synthase was observed adding an additional energy production pump. Proteins involved in the tricarboxylic acid (TCA) cycle and glycolysis were significantly upregulated in *M. thermoacetica*-CdS. Citrate and oxaloacetic acid stemming from acetyl-CoA are primary drivers of the TCA cycle. Finally, a part of glycolysis important for cell growth functions was activated. Notably, reducing equivalents can be produced from glycolysis and TCA cycle thus contributing to a host of cell functions.

### Cytoprotection

Photosensitization of microorganisms offers a promising platform for the light-driven catalytic conversion of CO<sub>2</sub>, N<sub>2</sub> and H<sub>2</sub>O into fuels

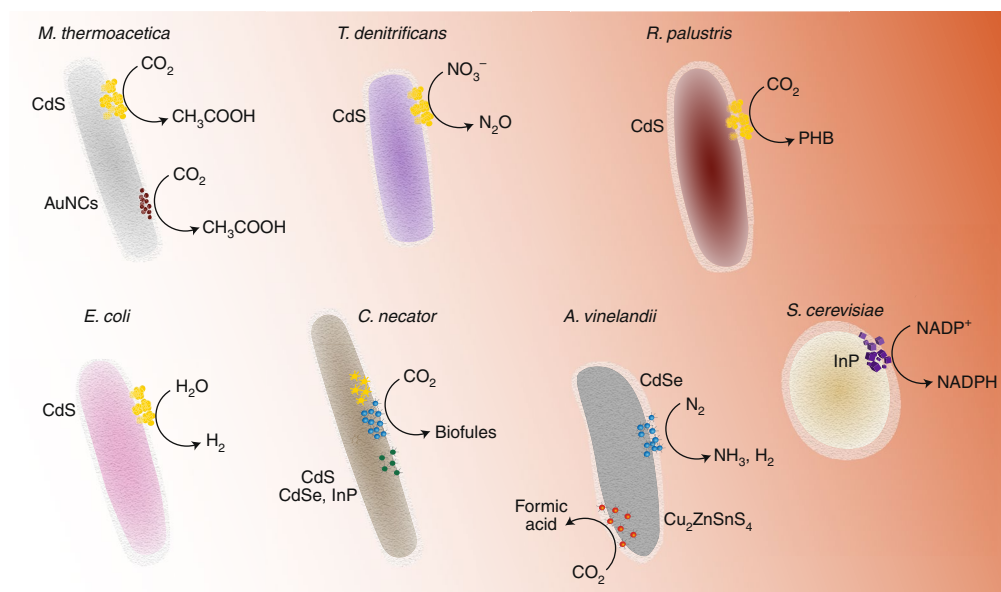


**Fig. 3 | Map of photosensitized microorganisms.** Photosensitizer–microorganism pairings enable the synthesis of carbon products (acetate, PHB, formic acid, biofuels),  $\text{H}_2$  and  $\text{NH}_3$  from  $\text{CO}_2$ ,  $\text{H}_2\text{O}$ ,  $\text{N}_2$  and light. The nanoparticles in *C. necator* and *A. vinelandii* incorporate a ZnS shell. InP nanoparticles photoregenerate NADPH in *S. cerevisiae*.

and value-added chemicals<sup>95</sup>. However, autotrophic organisms equipped with specialized metabolic pathways, such as *M. thermoacetica*, cannot sustain the high photon flux required for photosynthesis. In addition, enzymes responsible for reduction and hydrogenation like Rubisco, hydrogenase and nitrogenase are sensitive to oxygen<sup>96</sup>. Furthermore, sacrificial hole scavengers used to maximize charge separation of the photoexcited nanoparticles become depleted throughout the course of photosynthesis. Accordingly, a model strategy has been devised in which cystine is reduced back to cysteine by photoactive  $\text{TiO}_2$  nanocatalysts<sup>97</sup>. Although this approach boosts the overall yield of acetate from  $\text{CO}_2$  through an increase in the availability of cysteine, the photoanodic  $\text{TiO}_2$  nanocatalysts are also responsible for creating additional ROS (ref. <sup>98</sup>). In order to promote the applicability of photosensitized whole-cell organisms for solar-to-chemical conversion, it is imperative to devise of cytoprotective strategies to enable long-term stability even in oxidative environments.

Nature provides ample inspiration for cytoprotection. Diatoms, for instance, shield themselves with siliceous exoskeletons from environmental stressors<sup>99</sup>. Photosynthetic cyanobacteria extrude extracellular polymers that contain molecules absorbing in the UV range<sup>100</sup>. Therefore, approaches consisting of coating charged polymers<sup>101</sup>, inorganic materials<sup>102,103</sup> and metal–organic framework materials (MOFs)<sup>104</sup> directly onto cell membranes have provided protection against radiation, thermal and mechanical stresses<sup>105</sup>. As previously described hydrogenase-expressing *E. coli* was photosensitized with CdS nanoparticles for the solar-driven production of hydrogen<sup>80</sup>. Since hydrogenase is sensitive to oxygen, the *E. coli*–CdS biohybrids were encapsulated in silica. Conversely, charged polymers were deposited on the membrane of the cells thus offering scaffolding for silica synthesized from silicic acid. This enhancement resulted in the generation of a locally anaerobic microenvironment within the cell core, which allowed for the long-term stability of the photosynthetic biohybrids (Fig. 5a,b).

A further strategy consists of the complete encapsulation of a unit of photosensitized cells in a hydrogel. Alginate hydrogel, for

example, allows for the unencumbered proliferation of cells as its soft structure develops microvoids<sup>106</sup>. The alginate may scavenge and attenuate the concentration of superoxides, hypochlorites and peroxides<sup>107,108</sup>. *M. thermoacetica*–AuNCs encapsulation in hydrogel led to an increase in acetate produced during photosynthesis<sup>109</sup>.

MOFs are a class of microporous materials synthesized from modular building blocks that can be optimized to enhance biocompatibility<sup>110,111</sup>. Their exceptional thermal and chemical robustness have been shown to facilitate gas absorption with exemplary applications in mixed gas sequestration and  $\text{CO}_2$  electrocatalysis<sup>112,113</sup>. Liang and co-workers have demonstrated the in vitro precipitation of a zeolitic imidazolate framework (ZIF) on yeast<sup>104</sup>. The biomolecule-rich yeast membrane serves as a nucleation point for the ZIF when other precursors are present in the media. Remarkably, the crystallized ZIF prolongs the overall viability of yeast under adverse environments as shown in Fig. 5c. However, the stiff attachment of this material to the yeast membrane can prevent cell proliferation and induce dormant states. Additionally, this method may yield incomplete membrane coverage. Ji et al. developed a technique to uniformly wrap *M. thermoacetica* in flexible MOF nanosheets<sup>114</sup>. Phosphate residues on the cell surface act as anchoring points for zirconium clusters in the MOF nanosheets (Fig. 5d). Therefore, this ultrathin MOF material allows the mechanical dynamics required during cell division to occur. As compared to bare *M. thermoacetica*, the wrapped *M. thermoacetica* sustains a remarkably lower rate of inhibition when exposed to  $\text{H}_2\text{O}_2$ , a model ROS. The decomposition of ROS can be attributed to the catalytic ability of the zirconium clusters. Consequently, the MOF-wrapped *M. thermoacetica*–CdS can continuously undertake  $\text{CO}_2$  photoreduction even under oxidative stress, achieving a 200% increase in acetate yield over the bare biohybrids. Cytoprotection by MOF nanosheets containing zirconium clusters improves on the design of photosensitized organisms. This material allows for the creation of a complete cell factory, realizing artificial photosynthesis with simultaneous  $\text{CO}_2$  reduction and redox shuttle regeneration.



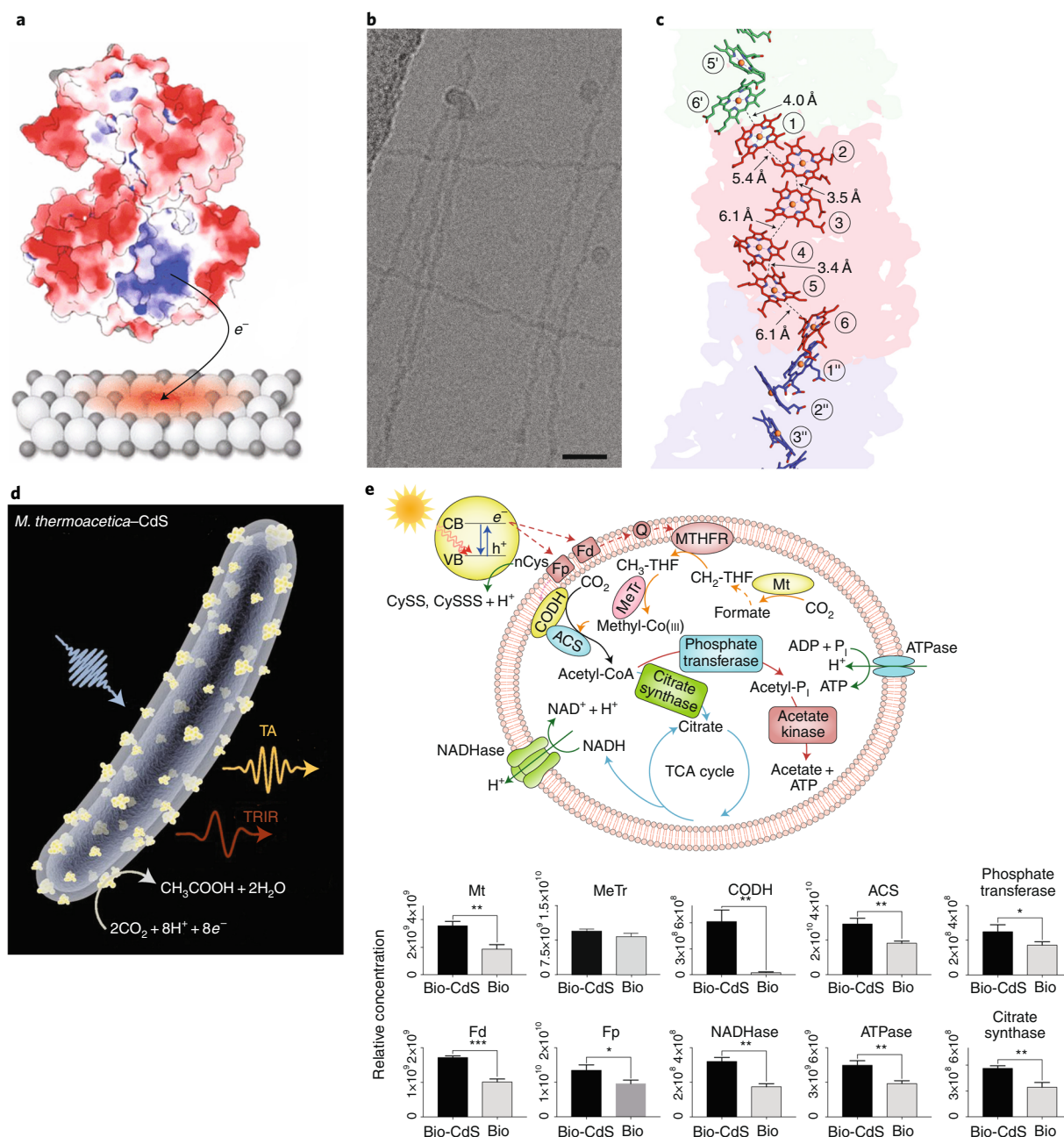


**Fig. 4 | Exploration of charge transfer mechanisms in microbial cells.** **a**, MtrF mediates electron transport on the membrane of *S. oneidensis* MR-1. **b**, Cryoelectron microscopy image depicting conducting microbial nanowires from *G. sulfurreducens* (scale bar, 200 Å). **c**, Scheme showing close-packed metal cluster haems in the core of microbial nanowires. **d**, Translucent *M. thermoacetica*-CdS hybrids allow for transient absorption (TA) and time-resolved infrared spectroscopy (TRIR). **e**, Proposed energy cascade in *M. thermoacetica*-CdS hybrids with relative abundances of its components as compared with non-photosensitized cells. Mt, formate dehydrogenase; MeTr, methyl-H4folate:CFeSP methyltransferase; CODH, CO dehydrogenase; ACS, acetyl-CoA synthase; Fd, ferredoxin; Fp, flavoprotein; NADHase, NADH dehydrogenase; ATPase, ATP synthase. Error bars represent the standard deviation. \* $P < 0.05$ ; \*\* $P < 0.01$ ; \*\*\* $P < 0.001$ . Three biological replicates were involved in each group. Figure adapted with permission from ref. <sup>89</sup>, American Chemical Society (a); ref. <sup>92</sup>, Elsevier (b,c); ref. <sup>93</sup>, PNAS (d); ref. <sup>94</sup>, Elsevier (e).

## Outlook

The coupling of whole-cell biocatalysts and semiconducting nanomaterials has allowed for the light-driven conversion of CO<sub>2</sub>, H<sub>2</sub>O and N<sub>2</sub> into value-added products. Research has centred around the biotic/abiotic interface, namely to create a functional flux of reducing equivalents either by direct electron transfer or through a mediator like H<sub>2</sub>. Although there have been significant developments in this field of research, there is room for improvement and challenges that need to be met.

Direct electron transfer to microorganisms is hindered by the change in pH of the microenvironment at the cathode and the relatively low extracellular electron transfer rate. The first limitation can be addressed by using a better buffering system and by designing an electrochemical cell with superior mass transport. Furthermore, upgrading from a primarily batch to a flow system could enhance biocompatibility. Flow-based microbial fuel cells with markedly improved performance have been reported<sup>115</sup>. With thorough understanding of extracellular electron transfer, bacteria

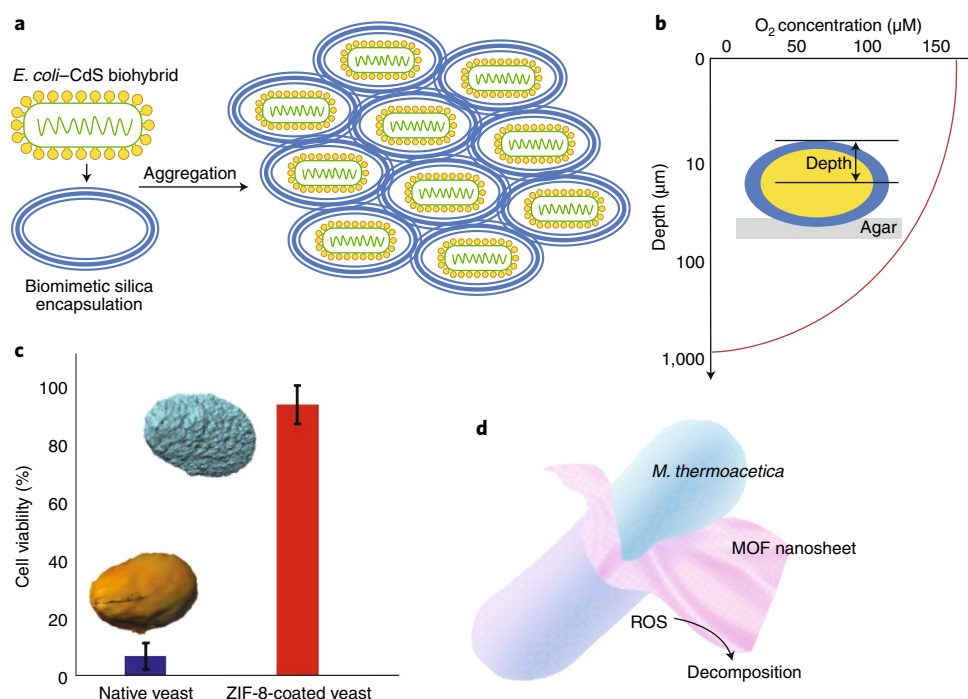


**Fig. 5 | Cytoprotective strategies for unicellular organisms.** **a**, *E. coli*-CdS biohybrids are encapsulated in silica shells to maintain a local anaerobic environment. **b**, Microsensor-based measurements display a sharp decrease in O<sub>2</sub> concentration with increasing depth. **c**, Schematic illustration of biomimetic crystallization of cytoprotective zeolitic imidazolate framework (ZIF) coatings on living cells. The bar graph indicates the culture viabilities (%) of native yeast (blue) and ZIF-coated yeast (red) under lysing conditions (3 h). **d**, Schematic of dynamic metal-organic framework (MOF) nanosheet covering *M. thermoacetica* while catalysing ROS decomposition. Figure adapted with permission from ref. <sup>80</sup>, AAAS (**b**); ref. <sup>104</sup>, Wiley (**c**).

could be genetically engineered to overexpress proteins responsible for charge uptake. This would greatly complement electrochemical adaptation studies. Non-electroactive workhorse bacteria with wide product arrays could even be engineered to accept charge. For instance, *S. cerevisiae* had not shown electroactivity but *S. cerevisiae*-InP hybrids successfully regenerated NADPH with light energy<sup>82</sup>. Moreover, microorganisms rarely exist in monocultures in nature. In fact, communities of organisms join forces to symbiotically exploit available sources of energy. Co-cultured organisms demonstrate synergistic effects as higher resiliency to stresses and overall increase in biomass<sup>116,117</sup>. Employing a diverse community of organisms can enhance the rate of microbial electrosynthesis as has been demonstrated<sup>118</sup>. Furthermore, a study by Lu and colleagues shows that bacterial communities derive photoexcited reducing equivalents from illuminated Mn and Fe oxides. This report provides an account of light-induced bacterial electrophory in nature and indicates that there is the need for further investigation into the synergistic relationship between light, cells and semiconducting materials. Furthermore, this research could provide the foundation for PEC semiconductor biohybrids with earth abundant oxides and a larger variety of biocatalysts.

Some of the highest current densities of microbial CO<sub>2</sub> reduction have been achieved by using H<sub>2</sub> as a reducing equivalent<sup>51</sup>. Taking this into consideration, solar power could provide the necessary energy to drive the hydrogen evolution reaction (HER) to power biocatalysts by coupling HER catalysts with light-absorbing materials. However, HER catalysts at the solid/liquid interface may obscure the semiconductor and thus decrease light harvesting. An alternative strategy consists of pairing a conventional photovoltaic device with an electrolyser. High (30%) solar-to-hydrogen efficiency has been attained by photovoltaic electrolysis systems<sup>119</sup>. Therefore, it stands to reason that producing more hydrogen efficiently could increase the total throughput of solar-based CO<sub>2</sub>

reduction. However, the challenge of maintaining a biocompatible environment persists. Fewer studies on N<sub>2</sub> assimilation by microbial electrosynthesis have surfaced. The reason for this might be that nitrogen-fixing bacteria quickly consume valuable NH<sub>3</sub>. Liu et al. were forced to inhibit protein biosynthesis in order to draw extracellular NH<sub>3</sub>. Therefore, nitrogenous biomass accumulation and NH<sub>3</sub> production could not be observed simultaneously. This points to a root challenge with microbial electrosynthesis—competition with biocatalysts for access to products may arise<sup>120</sup>.

Moreover, improvements on the biological aspect of semi-artificial photosynthesis are necessary to match advances on the bioinorganic interface. Electrochemical CO<sub>2</sub> reduction with inorganic catalysts can achieve CO<sub>2</sub> fixation with rates 10–50 times higher depending on the product<sup>14</sup>. The rate of carbon assimilation metabolism in autotrophic microorganisms needs to increase in order to compete with purely inorganic catalysts. This could be done through metabolic engineering of autotrophic organisms<sup>121</sup> or by constructing CO<sub>2</sub>-fixing pathways in highly active organisms such as *E. coli*<sup>122</sup>. Although whole-cell biocatalysts possess unrivalled selectivity of many desirable natural products and biofuels<sup>123</sup>, the yield and generation rate of these products needs to be optimized. This may be addressed by redesigning metabolic pathways<sup>124</sup>.

Photosensitized microorganisms have achieved direct solar-to-chemical conversion. However, most of these systems rely on hole scavengers. TiO<sub>2</sub> nanoparticles have been used to regenerate cysteine, a common scavenger. But as TiO<sub>2</sub> is intrinsically cytotoxic<sup>125</sup>, better approaches for scavenger regeneration are needed. Further in-depth study of the interaction between whole cells and light-active nanoparticles could provide more insight into the molecular pathway of charge uptake. Spectroscopic analyses could be combined with biochemical assays such as transposon sequencing<sup>126</sup>. Moreover, the field of nanocarrier-based drug delivery has solidified the paramount role of surface chemistry in nanomaterial–cell



interactions<sup>127</sup>. More exploration on the effect of surface chemistry of light-absorbing nanomaterials for photosensitization could continue to yield similarly interesting results.

Altogether, the union of biology and nanomaterials has shown promise to fulfill the mission of artificial photosynthesis. The illustrated biohybrid approaches play to the strengths of each component: the replication, self-healing and specificity of whole organisms and solar energy capture of semiconducting nanomaterials. The advent of photosynthetic semiconductor biohybrids has begun to enable conversion of sunlight into liquid fuels and value-added chemicals. With steady improvements, the prospect of engineered semiconductor nanomaterials enhancing the natural world may be realized.

Received: 17 July 2019; Accepted: 17 January 2020;

Published online: 18 March 2020

## References

- Sellers, P. J. et al. Comparison of radiative and physiological effects of doubled atmospheric CO<sub>2</sub> on climate. *Science* **271**, 1402–1406 (1996).
- Barber, J. Photosynthetic energy conversion: natural and artificial. *Chem. Soc. Rev.* **38**, 185–196 (2009).
- Lewis, N. S. Research opportunities to advance solar energy utilization. *Science* **351**, aad1920 (2016).
- Cook, T. R. et al. Solar energy supply and storage for the legacy and nonlegacy worlds. *Chem. Rev.* **110**, 6474–6502 (2010).
- Nelson, N. & Ben-Shem, A. The complex architecture of oxygenic photosynthesis. *Nat. Rev. Mol. Cell Biol.* **5**, 971–982 (2004).
- Williams, P. J. L. B. & Laurens, L. M. L. Microalgae as biodiesel & biomass feedstocks: review & analysis of the biochemistry, energetics & economics. *Energy Environ. Sci.* **3**, 554–590 (2010).
- Hill, J., Nelson, E., Tilman, D., Polasky, S. & Tiffany, D. Environmental, economic, and energetic costs and benefits of biodiesel and ethanol biofuels. *Proc. Natl Acad. Sci. USA* **103**, 11206–11210 (2006).
- Zhu, X.-G., Long, S. P. & Ort, D. R. Improving photosynthetic efficiency for greater yield. *Annu. Rev. Plant Biol.* **61**, 235–261 (2010).
- Green, M. A. et al. Solar cell efficiency tables (version 53). *Prog. Photovolt. Res. Appl.* **27**, 3–12 (2019).
- Blankenship, R. E. et al. Comparing photosynthetic and photovoltaic efficiencies and recognizing the potential for improvement. *Science* **332**, 805–809 (2011).
- Luo, J. et al. Water photolysis at 12.3% efficiency via perovskite photovoltaics and Earth-abundant catalysts. *Science* **345**, 1593–1596 (2014).
- Zhu, X. G., Long, S. P. & Ort, D. R. What is the maximum efficiency with which photosynthesis can convert solar energy into biomass? *Curr. Opin. Biotechnol.* **19**, 153–159 (2008).
- Mao, J., Li, K. & Peng, T. Recent advances in the photocatalytic CO<sub>2</sub> reduction over semiconductors. *Catal. Sci. Technol.* **3**, 2481–2498 (2013).
- Ross, M. B. et al. Designing materials for electrochemical carbon dioxide recycling. *Nat. Catal.* **2**, 648–658 (2019).
- Barton, E. E., Rampulla, D. M. & Bocarsly, A. B. Selective solar-driven reduction of CO<sub>2</sub> to methanol using a catalyzed p-GaP based photoelectrochemical cell. *J. Am. Chem. Soc.* **130**, 6342–6344 (2008).
- Sahara, G. et al. Photoelectrochemical Reduction of CO<sub>2</sub> coupled to water oxidation using a photocathode with a Ru(II)–Re(I) complex photocatalyst and a CoO<sub>3</sub>/TaON photoanode. *J. Am. Chem. Soc.* **138**, 14152–14158 (2016).
- Zhou, X. et al. Solar-driven reduction of 1 atm of CO<sub>2</sub> to formate at 10% energy-conversion efficiency by use of a TiO<sub>2</sub>-protected III–V tandem photoanode in conjunction with a bipolar membrane and a Pd/C cathode. *ACS Energy Lett.* **1**, 764–770 (2016).
- Bourzac, K. Liquid sunlight: fuels created by artificial photosynthesis are getting much closer to reality. *Proc. Natl Acad. Sci. USA* **113**, 4545–4548 (2016).
- Kim, D., Sakimoto, K. K., Hong, D. & Yang, P. Artificial photosynthesis for sustainable fuel and chemical production. *Angew. Chem. Int. Ed.* **54**, 3259–3266 (2015).
- Yoshikawa, K. et al. Silicon heterojunction solar cell with interdigitated back contacts for a photoconversion efficiency over 26%. *Nat. Energy* **2**, 17032 (2017).
- Chang, X., Wang, T. & Gong, J. CO<sub>2</sub> photo-reduction: insights into CO<sub>2</sub> activation and reaction on surfaces of photocatalysts. *Energy Environ. Sci.* **9**, 2177–2196 (2016).
- Kong, Q. et al. Directed assembly of nanoparticle catalysts on nanowire photoelectrodes for photoelectrochemical CO<sub>2</sub> reduction. *Nano Lett.* **16**, 5675–5680 (2016).
- Varela, A. S., Ju, W., Reier, T. & Strasser, P. Tuning the catalytic activity and selectivity of Cu for CO<sub>2</sub> electroreduction in the presence of halides. *ACS Catal.* **6**, 2136–2144 (2016).
- Das, A. & Ljungdahl, L. G. in *Biochemistry and Physiology of Anaerobic Bacteria* 191–204 (Springer, 2006).
- Liang, J.-Y. & Lipscomb, W. N. Binding of substrate CO<sub>2</sub> to the active site of human carbonic anhydrase II: a molecular dynamics study (zinc enzyme/binding pathway/enzyme-substrate interaction). *Proc. Natl Acad. Sci. USA* **87**, 3675–3679 (1990).
- Gray, H. B. & Winkler, J. R. Electron transfer in proteins. *Annu. Rev. Biochem.* **65**, 537–561 (1996).
- Cooney, M. J., Svoboda, V., Lau, C., Martin, G. & Minter, S. D. Enzyme catalysed biofuel cells. *Energy Environ. Sci.* **1**, 320–337 (2008).
- Schlager, S. et al. Electrochemical reduction of carbon dioxide to methanol by direct injection of electrons into immobilized enzymes on a modified electrode. *ChemSusChem* **9**, 631–635 (2016).
- Lamle, S. E., Vincent, K. A., Halliwell, L. M., Albracht, S. P. J. & Armstrong, F. A. Hydrogenase on an electrode: a remarkable heterogeneous catalyst. *J. Chem. Soc. Dalton Trans.* **3**, 4152–4157 (2003).
- Pinyou, P., Blay, V., Muresan, L. M. & Noguier, T. Enzyme-modified electrodes for biosensors and biofuel cells. *Mater. Horiz.* **6**, 1336–1358 (2019).
- Kornienko, N., Zhang, J. Z., Sakimoto, K. K., Yang, P. & Reisner, E. Interfacing nature's catalytic machinery with synthetic materials for semi-artificial photosynthesis. *Nat. Nanotechnol.* **13**, 890–899 (2018).
- Sarma, A. K., Vatsyayan, P., Goswami, P. & Minter, S. D. Recent advances in material science for developing enzyme electrodes. *Biosens. Bioelectron.* **24**, 2313–2322 (2009).
- Sakimoto, K. K. et al. Physical Biology of the Materials–Microorganism Interface. *J. Am. Chem. Soc.* **140**, 1978–1985 (2018).
- Rabaey, K. & Rozendal, R. A. Microbial electrosynthesis — revisiting the electrical route for microbial production. *Nat. Rev. Microbiol.* **8**, 706–716 (2010).
- Shi, L. et al. Extracellular electron transfer mechanisms between microorganisms and minerals. *Nat. Rev. Microbiol.* **14**, 651–662 (2016).
- Comprehensive review of active electron transfer pathways and mechanisms between microorganisms and inorganic minerals.**
- Nevin, K. P., Woodard, T. L., Franks, A. E., Summers, Z. M. & Lovley, D. R. Microbial electrosynthesis: feeding microbes electricity to convert carbon dioxide and water to multicarbon extracellular organic compounds. *mBio* **1**, e00103–10 (2010).
- Ragsdale, S. W. & Pierce, E. Acetogenesis and the Wood–Ljungdahl pathway of CO<sub>2</sub> fixation. *Biochim. Biophys. Acta* **1784**, 1873–1898 (2008).
- Aryal, N., Halder, A., Tremblay, P. L., Chi, Q. & Zhang, T. Enhanced microbial electrosynthesis with three-dimensional graphene functionalized cathodes fabricated via solvothermal synthesis. *Electrochim. Acta* **217**, 117–122 (2016).
- Su, L. & Ajo-Franklin, C. M. Reaching full potential: bioelectrochemical systems for storing renewable energy in chemical bonds. *Curr. Opin. Biotechnol.* **57**, 66–72 (2019).
- Zhang, T. et al. Improved cathode materials for microbial electrosynthesis. *Energy Environ. Sci.* **6**, 217–224 (2013).
- Tremblay, P. L., Höglund, D., Koza, A., Bonde, I. & Zhang, T. Adaptation of the autotrophic acetogen *Sporomusa ovata* to methanol accelerates the conversion of CO<sub>2</sub> to organic products. *Sci. Rep.* **5**, 16168 (2015).
- Marshall, C. W., Ross, D. E., Fichot, E. B., Norman, R. S. & May, H. D. Long-term operation of microbial electrosynthesis systems improves acetate production by autotrophic microbiomes. *Environ. Sci. Technol.* **47**, 6023–6029 (2013).
- Li, H. et al. Integrated electromicrobial conversion of CO<sub>2</sub> to higher alcohols. *Science* **335**, 1596 (2012).
- Liu, C. et al. Nanowire-bacteria hybrids for unassisted solar carbon dioxide fixation to value-added chemicals. *Nano Lett.* **15**, 3634–3639 (2015).
- This work demonstrates the ability to pair acetogenic microorganisms with light-active nanostructured electrodes for CO<sub>2</sub> reduction.**
- Shively, J. M., van Keulen, G. & Meijer, W. G. Something from almost nothing: carbon dioxide fixation in chemoautotrophs. *Annu. Rev. Microbiol.* **52**, 191–230 (1998).
- Wang, H. & Ren, Z. J. A comprehensive review of microbial electrochemical systems as a platform technology. *Biotechnol. Adv.* **31**, 1796–1807 (2013).
- Nichols, E. M. et al. Hybrid bioinorganic approach to solar-to-chemical conversion. *Proc. Natl Acad. Sci. USA* **112**, 11461–11466 (2015).
- Liu, C., Colón, B. C., Ziesack, M., Silver, P. A. & Nocera, D. G. Water splitting–biosynthetic system with CO<sub>2</sub> reduction efficiencies exceeding photosynthesis. *Science* **352**, 1210–1213 (2016).
- The authors present a highly energy efficient device consisting of self-regenerating non-toxic electrodes and CO<sub>2</sub>-fixing bacteria for production of bioplastics and biofuels.**
- Dogutan, D. K. & Nocera, D. G. Artificial photosynthesis at efficiencies greatly exceeding that of natural photosynthesis. *Acc. Chem. Res.* **52**, 3143–3148 (2019).

50. Liu, C., Sakimoto, K. K., Colón, B. C., Silver, P. A. & Nocera, D. G. Ambient nitrogen reduction cycle using a hybrid inorganic–biological system. *Proc. Natl Acad. Sci. USA* **114**, 6450–6455 (2017).
51. Rodrigues, R. M. et al. Perfluorocarbon nanoemulsion promotes the delivery of reducing equivalents for electricity-driven microbial CO<sub>2</sub> reduction. *Nat. Catal.* **2**, 407–414 (2019).
52. Quintana, N., Van Der Kooy, F., Van De Rhee, M. D., Voshol, G. P. & Verpoorte, R. Renewable energy from Cyanobacteria: Energy production optimization by metabolic pathway engineering. *Appl. Microbiol. Biotechnol.* **91**, 471–490 (2011).
53. Utschig, L. M., Soltan, S. R., Mulfort, K. L., Niklas, J. & Poluektov, O. G. Z-scheme solar water splitting: via self-assembly of photosystem I–catalyst hybrids in thylakoid membranes. *Chem. Sci.* **9**, 8504–8512 (2018).
54. Brown, K. A. et al. Light-driven dinitrogen reduction catalyzed by a CdS:nitrogenase MoFe protein biohybrid. *Science* **352**, 448–450 (2016).
55. Fast, A. G. & Papoutsakis, E. T. Stoichiometric and energetic analyses of non-photosynthetic CO<sub>2</sub>-fixation pathways to support synthetic biology strategies for production of fuels and chemicals. *Curr. Opin. Chem. Eng.* **1**, 380–395 (2012).
56. Sakimoto, K. K., Wong, A. B. & Yang, P. Self-photosensitization of nonphoto-synthetic bacteria for solar-to-chemical production. *Science* **351**, 74–77 (2016). **This work illustrates the concept of membrane-bound self-precipitated quantum dots to power CO<sub>2</sub> fixation of live whole-cell biocatalysts.**
57. Sweeney, R. Y. et al. Bacterial biosynthesis of cadmium sulfide nanocrystals. *Chem. Biol.* **11**, 1553–1559 (2004).
58. Oguri, T., Schneider, B. & Reitzer, L. Cysteine catabolism and cysteine desulfhydrase (CdsH/STM0458) in *Salmonella enterica* serovar typhimurium. *J. Bacteriol.* **194**, 4366–4376 (2012).
59. Drake, H. L. & Daniel, S. L. Physiology of the thermophilic acetogen *Moorella thermoacetica*. *Res. Microbiol.* **155**, 869–883 (2004).
60. Kloepper, J. A., Mielke, R. E. & Nadeau, J. L. Uptake of CdSe and CdSe/ZnS quantum dots into bacteria via purine-dependent mechanisms. *Appl. Environ. Microbiol.* **71**, 2548–2557 (2005).
61. Goldberg, M., Langer, R. & Jia, X. Nanostructured materials for applications in drug delivery and tissue engineering. *J. Biomater. Sci. Polym. Ed.* **18**, 241–268 (2007).
62. Wang, B., Jiang, Z., Yu, J. C., Wang, J. & Wong, P. K. Enhanced CO<sub>2</sub> reduction and valuable C<sub>2+</sub> chemical production by a CdS-photosynthetic hybrid system. *Nanoscale* **11**, 9296–9301 (2019).
63. Chen, M. et al. Light-driven nitrous oxide production via autotrophic denitrification by self-photosensitized *Thiobacillus denitrificans*. *Environ. Int.* **127**, 353–360 (2019).
64. Begg, S. L. et al. Dysregulation of transition metal ion homeostasis is the molecular basis for cadmium toxicity in *Streptococcus pneumoniae*. *Nat. Commun.* **6**, 6418 (2015).
65. Li, K. G. et al. Intracellular oxidative stress and cadmium ions release induce cytotoxicity of unmodified cadmium sulfide quantum dots. *Toxicol. Vitro* **23**, 1007–1013 (2009).
66. Godt, J. et al. The toxicity of cadmium and resulting hazards for human health. *J. Occup. Med. Toxicol.* **1**, 22 (2006).
67. Jin, R., Zeng, C., Zhou, M. & Chen, Y. Atomically precise colloidal metal nanoclusters and nanoparticles: fundamentals and opportunities. *Chem. Rev.* **116**, 10346–10413 (2016).
68. Zhou, M. et al. Three-orders-of-magnitude variation of carrier lifetimes with crystal phase of gold nanoclusters. *Science* **364**, 279–282 (2019).
69. Santiago-Gonzalez, B. et al. Permanent excimer superstructures by supramolecular networking of metal quantum clusters. *Science* **353**, 571–575 (2016).
70. Zhao, S. et al. Gold nanoclusters promote electrocatalytic water oxidation at the nanocluster/CoSe<sub>2</sub> interface. *J. Am. Chem. Soc.* **139**, 1077–1080 (2017).
71. Zeng, C. et al. Structural patterns at all scales in a nonmetallic chiral Au<sub>133</sub>(SR)<sub>52</sub> nanoparticle. *Sci. Adv.* **1**, e1500045 (2015).
72. Stampelcoskie, K. G. & Swint, A. Optimizing molecule-like gold clusters for light energy conversion. *J. Mater. Chem. A* **4**, 2075–2081 (2016).
73. Chen, Y. S., Choi, H. & Kamat, P. V. Metal-cluster-sensitized solar cells. A new class of thiolated gold sensitizers delivering efficiency greater than 2%. *J. Am. Chem. Soc.* **135**, 8822–8825 (2013).
74. Yu, Y. et al. Identification of a highly luminescent Au<sub>22</sub>(SG)<sub>18</sub> nanocluster. *J. Am. Chem. Soc.* **136**, 1246–1249 (2014).
75. Zhang, H. et al. Bacteria photosensitized by intracellular gold nanoclusters for solar fuel production. *Nat. Nanotechnol.* **13**, 900–905 (2018). **Demonstrates that biocompatible gold nanoclusters can be used to photosensitize CO<sub>2</sub>-fixing bacteria.**
76. Cestellos-Blanco, S., Zhang, H. & Yang, P. Solar-driven carbon dioxide fixation using photosynthetic semiconductor bio-hybrids. *Faraday Discuss.* **215**, 54–65 (2019).
77. Schuchmann, K. & Müller, V. Autotrophy at the thermodynamic limit of life: a model for energy conservation in acetogenic bacteria. *Nat. Rev. Microbiol.* **12**, 809–821 (2014).
78. Liu, T. & Khosla, C. Genetic engineering of *Escherichia coli* for biofuel production. *Annu. Rev. Genet.* **44**, 53–69 (2010).
79. Luo, X. et al. Complete biosynthesis of cannabinoids and their unnatural analogues in yeast. *Nature* **567**, 123–126 (2019).
80. Wei, W. et al. A surface-display biohybrid approach to light-driven hydrogen production in air. *Sci. Adv.* **4**, eaap9253 (2018). **The authors illustrate the use of cadmium sulfide quantum dots to provide hydrogenase within *E. coli* with reducing equivalents for H<sub>2</sub> production.**
81. Krassen, H. et al. Photosynthetic hydrogen production by a hybrid complex of photosystem I and [NiFe]-hydrogenase. *ACS Nano* **3**, 4055–4061 (2009).
82. Guo, J. et al. Light-driven fine chemical production in yeast biohybrids. *Science* **362**, 813–816 (2018). **In this study genetically modified yeast were enhanced with light-active indium phosphide nanoparticles in order to improve the production of shikimic acid.**
83. Ding, Y. et al. Nanorg microbial factories: light-driven renewable biochemical synthesis using quantum dot-bacteria nanobiohybrids. *J. Am. Chem. Soc.* **141**, 10272–10282 (2019). **This work broadly demonstrates that matching the band gap of semiconducting quantum dots with the redox potential of enzyme allows for efficient solar-to-chemical production.**
84. Lovley, D. R. & Nevin, K. P. Electrobiocommodities: powering microbial production of fuels and commodity chemicals from carbon dioxide with electricity. *Curr. Opin. Biotechnol.* **24**, 385–390 (2013).
85. Lovley, D. R. Electromicrobiology. *Annu. Rev. Microbiol.* **66**, 391–409 (2012).
86. Virdis, B. et al. Analysis of electron transfer dynamics in mixed community electroactive microbial biofilms. *RSC Adv.* **6**, 3650–3660 (2016).
87. Kracke, F., Vassilev, I. & Krömer, J. O. Microbial electron transport and energy conservation: the foundation for optimizing bioelectrochemical systems. *Front. Microbiol.* **6**, 575 (2015).
88. Light, S. H. et al. A flavin-based extracellular electron transfer mechanism in diverse Gram-positive bacteria. *Nature* **562**, 140–157 (2018).
89. Fukushima, T. et al. The molecular basis for binding of an electron transfer protein to a metal oxide surface. *J. Am. Chem. Soc.* **139**, 12647–12654 (2017).
90. Deutzmann, J. S., Sahin, M. & Spormann, A. M. Extracellular enzymes facilitate electron uptake in biocorrosion and bioelectrosynthesis. *mBio* **6**, e00496–15 (2015).
91. Reguera, G. et al. Extracellular electron transfer via microbial nanowires. *Nature* **435**, 1098–1101 (2005).
92. Wang, F. et al. Structure of microbial nanowires reveals stacked hemes that transport electrons over micrometers. *Cell* **177**, 361–369 (2019).
93. Kornienko, N. et al. Spectroscopic elucidation of energy transfer in hybrid inorganic-biological organisms for solar-to-chemical production. *Proc. Natl Acad. Sci. USA* **113**, 11750–11755 (2016). **Determined that photosensitized bacteria exhibit spectroscopic changes that allow the authors to propose charge transfer pathways.**
94. Zhang, R. et al. Proteomic and metabolic elucidation of solar-powered biomanufacturing by bio-abiotic hybrid system. *Chem* **6**, P234–249 (2019). **This study elucidates charge transfer mechanisms of photosensitized bacteria by examining proteomics and metabolomics.**
95. Sakimoto, K. K., Kornienko, N. & Yang, P. Cyborgian material design for solar fuel production: the emerging photosynthetic biohybrid systems. *Acc. Chem. Res.* **50**, 476–481 (2017).
96. Lambert, C. et al. O<sub>2</sub> reactions at the six-iron active site (H-cluster) in [FeFe]-hydrogenase. *J. Biol. Chem.* **286**, 40614–40623 (2011).
97. Sakimoto, K. K., Zhang, S. J. & Yang, P. Cysteine-cysteine photoregeneration for oxygenic photosynthesis of acetic acid from CO<sub>2</sub> by a tandem inorganic-biological hybrid system. *Nano Lett.* **16**, 5883–5887 (2016).
98. Hirakawa, K., Mori, M., Yoshida, M., Oikawa, S. & Kawanishi, S. Photo-irradiated titanium dioxide catalyzes site specific DNA damage via generation of hydrogen peroxide. *Free Radic. Res.* **38**, 439–447 (2004).
99. Mishra, M., Arukha, A. P., Bashir, T., Yadav, D. & Prasad, G. B. K. S. All new faces of diatoms: potential source of nanomaterials and beyond. *Front. Microbiol.* **8**, 1239 (2017).
100. Ehling-Schulz, M. & Scherer, S. UV protection in cyanobacteria. *Eur. J. Phycol.* **34**, 329–338 (1999).
101. Shchukin, D. G., Shutava, T., Shchukina, E., Sukhorukov, G. B. & Lvov, Y. M. Modified polyelectrolyte microcapsules as smart defense systems. *Chem. Mater.* **16**, 3446–3451 (2004).
102. Yang, S. H., Ko, E. H. & Choi, I. S. Cyto-compatible encapsulation of individual chlorella cells within titanium dioxide shells by a designed catalytic peptide. *Langmuir* **28**, 2151–2155 (2012).
103. Yang, S. H. et al. Biomimetic encapsulation of individual cells with silica. *Angew. Chem. Int. Ed.* **48**, 9160–9163 (2009).
104. Liang, K. et al. Metal–organic framework coatings as cytoprotective exoskeletons for living cells. *Adv. Mater.* **28**, 7910–7914 (2016).

105. Park, J. H. et al. Nanocoating of single cells: from maintenance of cell viability to manipulation of cellular activities. *Adv. Mater.* **26**, 2001–2010 (2014).
106. Allan-Wojtas, P., Truelstrup Hansen, L. & Paulson, A. T. Microstructural studies of probiotic bacteria-loaded alginate microcapsules using standard electron microscopy techniques and anhydrous fixation. *LWT Food Sci. Technol.* **41**, 101–108 (2008).
107. Thankam Finosh, G. & Jayabalan, M. Reactive oxygen species—Control and management using amphiphilic biosynthetic hydrogels for cardiac applications. *Adv. Biosci. Biotechnol.* **4**, 1134–1146 (2013).
108. Kim, B. J. et al. Control of microbial growth in alginate/polydopamine core/shell microbeads. *Chem. Asian J.* **10**, 2130–2133 (2015).
109. Cestellos-Blanco, S., Zhang, H. & Yang, P. Solar-driven carbon dioxide fixation using photosynthetic semiconductor bio-hybrids. *Faraday Discuss.* **215**, 54–65 (2019).
110. Zhou, H.-C., Long, J. R. & Yaghi, O. M. Introduction to metal–organic frameworks. *Chem. Rev.* **112**, 673–674 (2012).
111. Liang, K. et al. An enzyme-coated metal–organic framework shell for synthetically adaptive cell survival. *Angew. Chem. Int. Ed.* **56**, 8510–8515 (2017).
112. Zhan, W. et al. Semiconductor@metal–organic framework core–shell heterostructures: a case of ZnO@ZIF-8 nanorods with selective photoelectrochemical response. *J. Am. Chem. Soc.* **135**, 1926–1933 (2013).
113. Kornienko, N. et al. Metal–organic frameworks for electrocatalytic reduction of carbon dioxide. *J. Am. Chem. Soc.* **137**, 14129–14135 (2015).
114. Ji, Z., Zhang, H., Liu, H., Yaghi, O. M. & Yang, P. Cytoprotective metal–organic frameworks for anaerobic bacteria. *Proc. Natl Acad. Sci. USA* **115**, 10582–10587 (2018).
- A two-dimensional zirconium-based MOF nanosheet can be used to protect bacteria from oxygen and ROS.**
115. Robertson, S. J., Grattieri, M., Behring, J., Bestetti, M. & Minter, S. D. Transitioning from batch to flow hypersaline microbial fuel cells. *Electrochim. Acta* **317**, 494–501 (2019).
116. Smith, M. J. & Francis, M. B. A designed *A. vinelandii*–*S. elongatus* coculture for chemical photoproduction from air, water, phosphate, and trace metals. *ACS Synth. Biol.* **5**, 955–961 (2016).
117. Angelis, S. et al. Co-culture of microalgae, cyanobacteria, and macromycetes for exopolysaccharides production: process preliminary optimization and partial characterization. *Appl. Biochem. Biotechnol.* **167**, 1092–1106 (2012).
118. Marshall, C. W., Ross, D. E., Fichot, E. B., Norman, R. S. & May, H. D. Electrosynthesis of commodity chemicals by an autotrophic microbial community. *Appl. Environ. Microbiol.* **78**, 8412–8420 (2012).
119. Jia, J. et al. Solar water splitting by photovoltaic-electrolysis with a solar-to-hydrogen efficiency over 30%. *Nat. Commun.* **7**, 13237 (2016).
120. McNeely, K., Xu, Y., Bennette, N., Bryant, D. A. & Dismukes, G. C. Redirecting reductant flux into hydrogen production via metabolic engineering of fermentative carbon metabolism in a cyanobacterium. *Appl. Environ. Microbiol.* **76**, 5032–5038 (2010).
121. Atsumi, S., Higashide, W. & Liao, J. C. Direct photosynthetic recycling of carbon dioxide to isobutyraldehyde. *Nat. Biotechnol.* **27**, 1177–1180 (2009).
122. Antonovsky, N. et al. Sugar synthesis from CO<sub>2</sub> in *Escherichia coli*. *Cell* **166**, 115–125 (2016).
123. Kung, Y., Runguphan, W. & Keasling, J. D. From fields to fuels: recent advances in the microbial production of biofuels. *ACS Synth. Biol.* **1**, 498–513 (2012).
124. Liao, J. C., Mi, L., Pontrelli, S. & Luo, S. Fuelling the future: microbial engineering for the production of sustainable biofuels. *Nat. Rev. Microbiol.* **14**, 288–304 (2016).
125. Lu, Z.-X. et al. Cell damage induced by photocatalysis of TiO<sub>2</sub> thin films. *Langmuir* **19**, 8765–8768 (2003).
126. Chan, C. H., Levar, C. E., Jiménez-Otero, F. & Bond, D. R. Genome scale mutational analysis of geobacter sulfurreducens reveals distinct molecular mechanisms for respiration and sensing of poised electrodes versus Fe(III) oxides. *J. Bacteriol.* **199**, e00340–17 (2017).
127. Ha, C.-S. & Gardella, J. A. Surface chemistry of biodegradable polymers for drug delivery systems. *Chem. Rev.* **105**, 4205–4232 (2005).

## Acknowledgements

This work was supported by NASA, Center for the Utilization of Biological Engineering in Space, under award NNX17AJ31G. S.C.-B. acknowledges a fellowship from the Philomathia Foundation. H.Z. is supported by the Suzhou Industry Park Fellowship and J.M.K. is supported by the Kwanjeong Educational Foundation.

## Competing interests

The authors declare no competing interests.

## Additional information

Correspondence should be addressed to P.Y.

Reprints and permissions information is available at [www.nature.com/reprints](http://www.nature.com/reprints).

**Publisher's note** Springer Nature remains neutral with regard to jurisdictional claims in published maps and institutional affiliations.

© Springer Nature Limited 2020